



Evidence from Fermi surface analysis for the low-temperature structure of lithium

Sabri F. Elatresh^a, Weizhao Cai^b, N. W. Ashcroft^c, Roald Hoffmann^{a,1}, Shanti Deemyad^{b,1}, and Stanimir A. Bonev^{d,1}

^aDepartment of Chemistry and Chemical Biology, Cornell University, Ithaca, NY 14853; ^bDepartment of Physics and Astronomy, University of Utah, Salt Lake City, UT 84112; ^cLaboratory of Atomic and Solid State Physics, Cornell University, Ithaca, NY 14853; and ^dLawrence Livermore National Laboratory, Livermore, CA 94550

Contributed by Roald Hoffmann, April 10, 2017 (sent for review February 6, 2017; reviewed by Jeffrey B. Neaton and James S. Schilling)

The low-temperature crystal structure of elemental lithium, the prototypical simple metal, is a several-decades-old problem. At 1 atm pressure and 298 K, Li forms a body-centered cubic lattice, which is common to all alkali metals. However, a low-temperature phase transition was experimentally detected to a structure initially identified as having the 9R stacking. This structure, proposed by Overhauser in 1984, has been questioned repeatedly but has not been confirmed. Here we present a theoretical analysis of the Fermi surface of lithium in several relevant structures. We demonstrate that experimental measurements of the Fermi surface based on the de Haas–van Alphen effect can be used as a diagnostic method to investigate the low-temperature phase diagram of lithium. This approach may overcome the limitations of X-ray and neutron diffraction techniques and makes possible, in principle, the determination of the lithium low-temperature structure (and that of other metals) at both ambient and high pressure. The theoretical results are compared with existing low-temperature ambient pressure experimental data, which are shown to be inconsistent with a 9R phase for the low-temperature structure of lithium.

lithium | Fermi surface | de Haas–van Alphen effect | low temperature | crystal structure

The behavior of the alkali metals under pressure has been a subject of considerable interest because of the emergence of unexpected physical properties (1–9). Lithium presents the simplest electronic structure of a metal under ambient conditions—a model for a nearly free electron crystal, with a simple and highly symmetric body-centered cubic (*bcc*) structure. Under application of external pressure, lithium undergoes a series of structural transitions to complex low-symmetry phases (3, 8, 10). These structural transformations are coupled with changes of its electronic properties, leading to a deviation from simple metallic behavior, including a complex phase diagram, a dramatic change in the superconducting T_c , metal–semiconductor phase transitions, as well as an anomalous melting curve (1, 4, 5, 10–14). Despite its apparent simplicity and numerous studies, there are still many open questions regarding the properties of lithium, even at $P = 1$ atm.

Among the outstanding questions is the structure of Li at low temperature and pressure. At 1 atm and 298 K lithium crystallizes in the *bcc* phase. However, upon cooling it undergoes a martensitic transformation that commences at ~ 80 K. Identifying the phases involved in the martensitic transition of lithium has been a challenge since its initial discovery (15). This has been due to several factors, including relatively poor response of lithium to both X-rays and neutrons; incomplete transition to the lowest measured temperature; and dependence of the transition temperature on multiple factors such as grain size, defects, and strain. The transition was first reported by C. S. Barrett (15, 16). Initial neutron scattering data by McCarthy et al. (17) identified the posttransition structure as hexagonal close-packed (*hcp*), but later Overhauser (18) suggested a rhombohedral structure with the 9R stacking for the low-temperature phase, based on analysis of neutron scattering data. The proposed 9R lithium struc-

ture is composed of nine hexagonal layers with stacking order ABCBCACAB; it is a close-packed phase yet different from the common face-centered cubic (*fcc*) and hexagonal close-packed *hcp*. Subsequent elastic neutron measurements (19, 20) on Li single crystals confirmed the appearance of Bragg reflections corresponding to both 9R and *fcc* phases, together with a considerable amount of diffuse scattering and some unidentified diffraction peaks. However, based on diffuse neutron scattering studies (21), it was also suggested that Li could form a disordered polytype at low temperature, where various close-packed stacking sequences (e.g., of the *hcp*, *fcc*, and 9R types) are all simultaneously present. Upon heating, the disordered polytype enters an *fcc* phase before reverting to a single crystal with the same *bcc* orientation as that found above 150 K (19, 21). Above 100 K, isothermal compression of lithium leads to direct transformation of *bcc* to *fcc* (2, 9, 22).

Most theoretical studies of the $P = 1$ atm lithium phases to date have been limited to ground-state static lattices ($T \rightarrow 0$ K); some even neglect the zero-point energy computed in a harmonic approximation (23–25). As a consequence, conflicting conclusions have been reached for the low-temperature structure of lithium. Nevertheless, there is general agreement that the enthalpy differences between competing lithium structures are exceedingly small (less than 2 meV per atom). Staikov et al. (25) included lattice dynamics within the harmonic approximation but found that the difference between the Helmholtz free energies of *bcc* and the closed-packed structures remains small in the temperature range of interest. Liu et al. (26) included the volume dependence of the phonon frequencies within a

Significance

Metals often take on simple close-packed structures. For what is arguably the simplest metal, lithium, there has been a controversy as to its low-temperature equilibrium structure, with a certain close-packed structure, 9R, long suggested. We propose a way to get further information about the structure when the most useful crystallographic methods are for one or another reason not applicable. This is to measure oscillations of the crystal magnetic moment of a material, the de Haas–van Alphen effect. The resulting spectrum of resonances relates directly to the Fermi surface of the metal and is quite distinctive for different structures. Using this methodology, we reason that the low-temperature crystal structure of lithium is not the heretofore assigned 9R structure.

Author contributions: S.D. and S.A.B. designed research; S.F.E., W.C., S.D., and S.A.B. performed research; S.F.E., W.C., N.W.A., R.H., S.D., and S.A.B. analyzed data; and S.F.E., W.C., R.H., S.D., and S.A.B. wrote the paper.

Reviewers: J.B.N., University of California, Berkeley; and J.S.S., Washington University in St. Louis.

The authors declare no conflict of interest.

¹To whom correspondence may be addressed. Email: rh34@cornell.edu, deemyad@physics.utah.edu, or bonev@llnl.gov.

This article contains supporting information online at www.pnas.org/lookup/suppl/doi:10.1073/pnas.1701994114/-DCSupplemental.

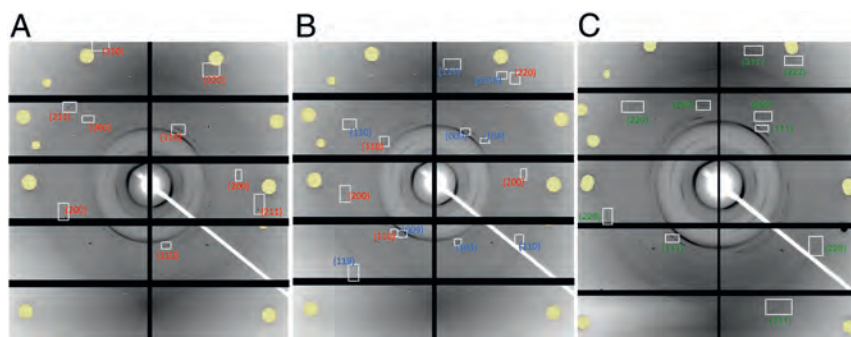


Fig. 1. Diffraction images of ${}^7\text{Li}$ at various temperatures and pressures: (A) room temperature (RT) and 2.8 GPa, (B) 20 K and 2.8 GPa, and (C) 20 K and 5.2 GPa. Diffraction from different phases is marked by white squares and accompanied by their hkl indices. Red, blue, and green show the hkl indices for bcc , $9R$, and fcc , respectively. The diamond reflections are marked by large yellow spots. The inner powder rings [low-angle diffraction peaks below bcc (110)] are reflections from the Cryostat window (Kapton film).

quasi-harmonic approximation with similar conclusion. It is clear that determining the low- T state of lithium based on energetic calculations alone is practically impossible at this stage or, if the small calculated free energy differences are accompanied by small barriers, that solid Li at low temperature and pressure is a dynamical system, with structures possibly dependent on mode of preparation.

In this paper we propose an alternative approach for determining the structure of low-temperature phases of lithium that attempts to circumvent both the theoretical and experimental difficulties. The strategy is based on the observation that a transition from the simple-metal monatomic fcc and bcc phases to a lower-symmetry one (such as $9R$) is accompanied by a dramatic deformation of the lithium Fermi surface (FS). This, in turn, can be clearly distinguished by a de Haas-van Alphen (dHvA) effect measurement (to be described in detail below). This approach is applicable at 1 atm, as well as to higher-pressure structures, where resolving the complex structures from neutron or X-ray diffraction data becomes even more difficult. In this paper we have applied this approach at 1 atm pressure and show that existing measurements are inconsistent with the $9R$ phase geometry's being the low-temperature state structure of lithium. Furthermore, the reported theoretical results can be used to draw stronger conclusions from future experiments that use either single crystal or polycrystalline samples.

Results

X-Ray Diffraction Analysis. First, we illustrate the difficulties in determining the low- T state structure of Li using conventional X-ray.

Fig. 1 shows representative diffraction patterns of bcc , $9R$, and fcc phases of lithium collected using high-resolution micro X-ray crystallography at the synchrotron facility (*Methods*). For simplicity, here we will refer to the low-temperature phase as $9R$ even though this identification is put into question in what follows. These patterns were collected first during isobaric cooling from RT \rightarrow 20 K at 2.8 GPa, followed by isothermal compression at 20 K from 2.8 GPa to 4.8 GPa. The paths correspond to a hypothetical structural phase transition from $bcc \rightarrow 9R + bcc$, and $9R + bcc \rightarrow fcc$, respectively. The appearance of new diffraction peaks can be clearly seen between Fig. 1 A and B, showing a structural phase transition during cooling. However, it is obvious that the quality of data does not allow refinement of the structure. In part this is the result of the limitation in angular access to the sample through the diamond windows of the cell, which prevents collecting data from all possible directions.

Metals in general are highly susceptible to forming texture or preferred orientation. During low-temperature pressure-

induced structural phase transitions these effects are usually amplified and all of the Bragg peaks from the new structure may not be present in the diffraction pattern. Moreover, there is difficulty performing single crystal studies concurrently at low temperature and high pressure. Therefore, most studies under such conditions are done using powder X-ray diffraction methods, which are less accurate than measurement on single crystals. Here theory can be of use; in the case at hand, the structures of lithium are assigned by comparing the observed diffraction pattern to those of known or predicted (10, 17, 18) structures for lithium. In Fig. 2 such a comparison for the four potential structures is shown. Based on this approach, certain structures can be excluded. However, due to lack of sufficient resolution, assurance in determination of the structure would require complementary information.

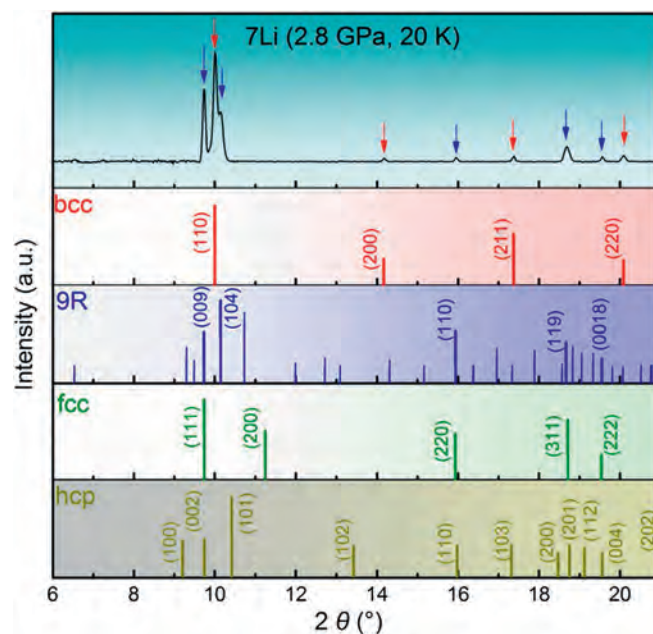


Fig. 2. X-ray diffraction pattern of ${}^7\text{Li}$ collected at 20 K and 2.8 GPa using a 30.5-keV X-ray beam ($\lambda = 0.4066 \text{ \AA}$). The corresponding diffraction patterns for different structures are plotted on the panels below. Heavier lines are the peaks that could be observed in the diffraction pattern of the sample. The cryostat has a background that does not shift with pressure. For clarity, the Compton scattering of the diamonds and reflections from the cryostat window have been removed. Red and blue arrows indicate reflections from bcc and $9R$ phases, respectively. a.u., arbitrary units.

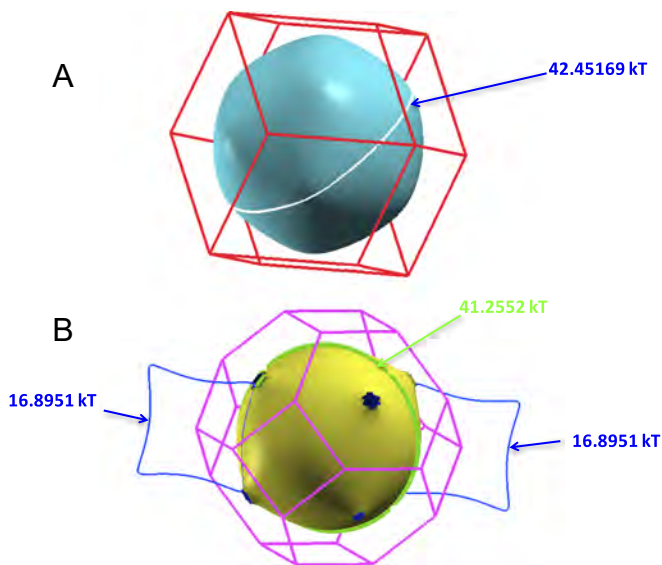


Fig. 3. BZ, FS, its extremal orbits, and their frequencies for (A) *bcc* and (B) *fcc* Li computed in its ground state at $P = 1$ atm.

In addition to the low-pressure martensitic transition, lithium undergoes a series of structural phase transitions at higher pressure to lower symmetry phases (1, 3, 8, 10). Determination of these structures also relies heavily on calculations, and alternative structures cannot be excluded based on diffraction studies. Moreover, as we mentioned earlier, the exceedingly small energetic differences between competitive structures makes determination of the relative stability of all candidate geometries practically impossible.

FS Analysis. As an alternative method for structure determination of Li at low temperature, which can be applied to other metals as well, we propose identifying the structures based on the geometry of their FSs, which are both theoretically and experimentally accessible. Because the Brillouin zone (BZ) of *9R* differs significantly from that of *bcc* and *fcc*, we expect that their FSs are easily distinguishable. In fact, even small shifts of the FS relative to the BZ boundaries can lead to measurable deformations of the FS. The calculated FSs of *bcc* and *fcc* lithium at 1 atm pressure are shown in Fig. 3. Whereas the former is nearly spherical, the BZ boundaries of *fcc* come slightly closer to the FS (the reciprocal lattice of *fcc* is *bcc*, which is not, strictly speaking, close-packed). This is sufficient to cause a noticeable deformation—the appearance of “necks” at the BZ boundaries.

Experimentally, information about the geometry of the FS can be obtained using Shubnikov–de Haas or dHvA effect studies (27). These effects are the oscillation of the electrical resistivity and the diamagnetic susceptibility of a crystal as the strength of an applied magnetic field varies. The effect, which has a venerable history, is due the Landau quantization of electron orbits in metals. The measured period of oscillations of the crystal magnetic moment plotted versus $1/H$, where H is the applied magnetic field, is proportional to the inverse of the extremal (maximum or minimum) cross-section of the FS normal to H .

For a nearly spherical FS, like that of *bcc* Li, the extremal orbits for any orientation of H are practically identical (Fig. 3A). In *fcc*, however, because the FS is deformed the extremal orbits for certain magnetic field orientations pass through the FS necks (Fig. 3B), which have very different areas. The period of oscillations of these orbits (commonly expressed in units of kilotesla) is the characteristic that clearly distinguishes the two phases.

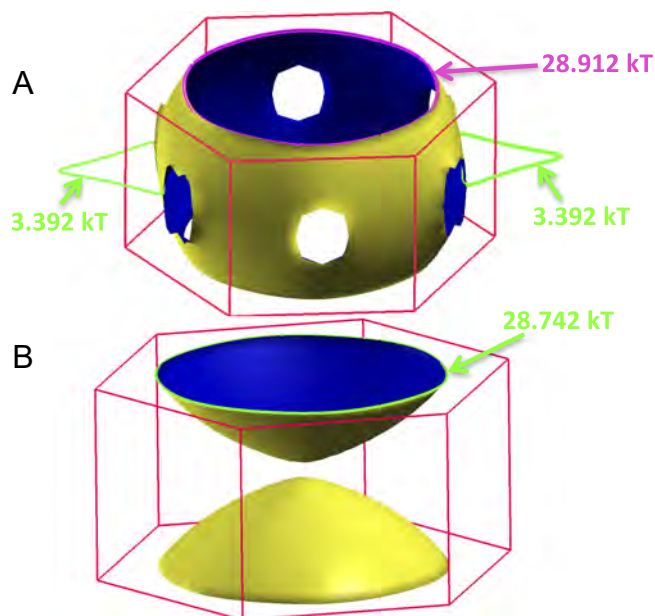


Fig. 4. BZ, FS, selected extremal orbits, and their frequencies for *hcp* Li computed in its ground state at $P = 1$ atm. Here A and B show separately the FSs originating from bands 3 and 4, respectively. The band structure, with band numbering, is shown in *SI Appendix, Fig. S3*.

Because the *hcp* and *9R* structures are not monatomic they have multiple electron bands crossing the Fermi level. The resulting complicated FSs, consisting of several pieces, are shown in Figs. 4 and 5. For any orientation of the magnetic field there are multiple extremal orbits with significantly different areas and dHvA frequencies (selected symmetric orbits and their frequencies are illustrated in Figs. 3–5). Importantly, a phase transition away from *bcc* or *fcc* can be detected unambiguously with an experimental setup using either poly- or single-crystalline samples, and independent of the orientation of the magnetic field with respect to the crystal.

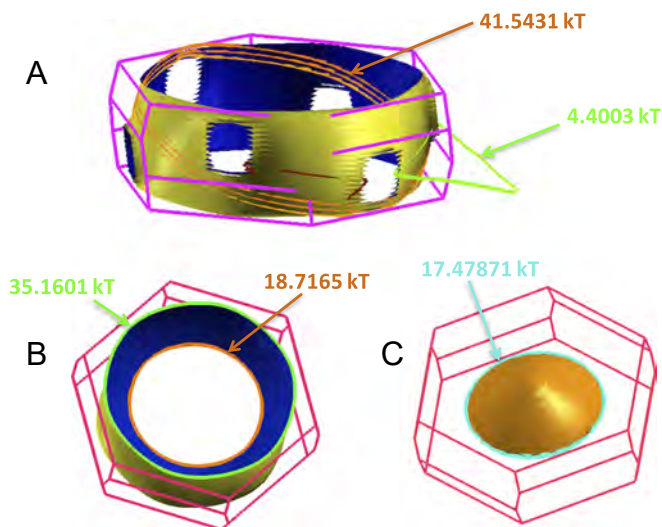


Fig. 5. BZ, FS, selected extremal orbits, and their frequencies for the *9R* structure of Li computed in its ground state at $P = 1$ atm. Here A, B, and C show the surfaces originating from bands 4, 5, and 6, respectively. The bands are indicated in *SI Appendix, Fig. S5*.

To identify $9R$ it is necessary to be able to distinguish it from hcp and other structures with complex FSs that may be competitive at low temperature. For this purpose, measurements of the dHvA frequencies for different magnetic field orientations are required. In Fig. 6 we report computed dHvA frequencies for $9R$ for selected θ angles and ϕ varied continuously between 0 and 180° (see Fig. 6 legend for the definition of the polar angles θ and ϕ , which specify the orientation of the magnetic field with respect to the BZ). These data can be used together with magnetic measurements on single-crystal Li samples to uniquely identify the presence of $9R$. Note specifically the continuous spectrum of high-frequency orbits originating from band 5, which are characteristic for $9R$. They exist because of the cylindrical shape of the FS due to band 5 (Fig. 5B).

In an experimental setup, for various reasons (e.g., the loss of single crystal character due to application of pressure or during structural phase transitions) the sample may not be single-crystal, but polycrystalline or powder. In such cases, the orientation of the magnetic field with respect to the crystal geometry is unspecified. To compare the theoretical results with measurements in such cases we have created a histogram of dHvA frequencies for the relevant structures, where we have considered all possible orientations of the magnetic field with respect to the respective BZs. The results are reported in Fig. 7 for angles ϕ from 0° to 180° and θ from 0° to 360° and the dHvA frequencies are collected in bins of size 0.05 kT. We confirm that for bcc all dHvA frequencies indeed aggregate around a single frequency of about 42 kT. Compared with it, fcc is indistinguishable, except for a peak near 17 kT, a distribution of frequencies near 5 kT, and a slight broadening of the histogram peak at 42 kT. In contrast, hcp and $9R$ have an almost continuous spectrum of dHvA frequencies, which distinguishes them easily from the monoatomic structures. In *SI Appendix*, Fig. S8 we show the sensitivity of the FS and calculated dHvA spectrum to lattice spacings (thus pressure).

It should be noted that although the amplitude of the dHvA oscillations from polycrystalline samples is significantly smaller, a residual amplitude, which is quite detectable, is still expected (as evident from Fig. 8, where the oscillations from the Cu coil are seen). Furthermore, the spectrum of $9R$ extends to much higher frequencies (>50 kT), as well as having multiple very-low-frequency (<3 kT) orbits, which is sufficient to identify it uniquely.

Discussion

Our theoretical results can be compared with existing measurements. The latest available Fermiology data (28) on lithium are shown in Fig. 8. According to the analysis we showed above, in the presence of even partial phase transition to $9R$ there should be quantum oscillations different from the ones seen in these data. Specifically, $9R$ has several characteristic frequencies below 12 kT (the peaks in Fig. 7), which should be observed in any geometric setup. Additional dHvA oscillations with higher frequencies, more strongly dependent on orientation, would also be present if the structure were $9R$. The absence of these features from the experimental data strongly suggests that $9R$ is not the structure of Li at these conditions. We note the hcp must be ruled out based on similar arguments.

It had been originally thought that because of the small size of the grain samples used in the measurements (~ 200 μm diameter) bcc does not transform to the low-temperature martensitic structure. However, recent X-ray data illustrated in Fig. 1 show that a structural phase transition in a similar-size sample (~ 100 μm diameter) clearly takes place at low temperature. The absence of $9R$ peaks in the dHvA data cannot be explained by size-dependence arguments. We emphasize that a transition to $9R$ even in only a few of the (larger) grains would have been evident in the dHvA data. At the temperatures where

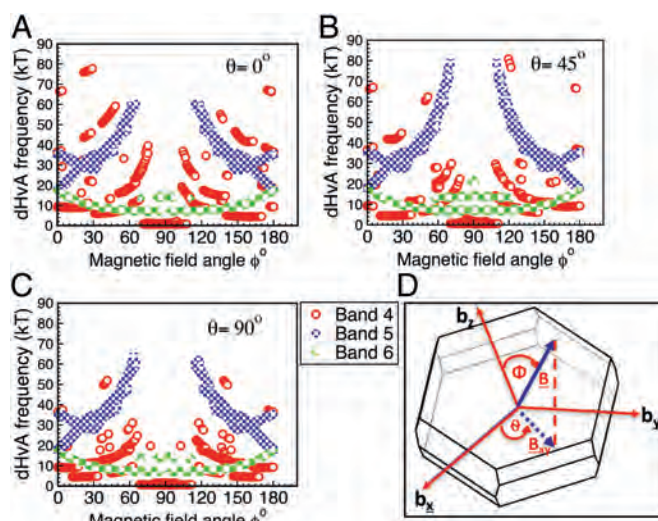


Fig. 6. Computed dHvA frequencies for Li in the $9R$ structure. The angle ϕ is varied continuously, whereas θ is fixed at (A) 0° , (B) 90° , or (C) 45° . The definition of θ and ϕ with respect to the BZ $9R$ and reciprocal lattice vectors is shown schematically in D.

the dHvA measurements are performed, over 75% of the sample is expected to be transformed to martensitic form.

We note that the dHvA frequencies that distinguish bcc and fcc are not seen in the experimental data (Fig. 8). They correspond to orbits that pass through the necks of the fcc FS and are observed only at specific crystal-magnetic field orientations. Therefore, despite their absence, ruling out fcc definitively is not possible without knowing the full details of the experimental setup or how the data have been analyzed.

In summary, the low-temperature crystal structure of Li at 1 atm as well as at higher pressure is a long-standing open problem. We illustrated the difficulties in resolving this matter using standard measurement techniques, such as X-ray diffraction. However, Fermiology measurements can be used as a complementary probe to help determine the low- T state of Li. Our theoretical calculations show that a transition from bcc —even partial—has a clear signature in the dHvA frequencies. This signature can be seen regardless of the magnetic orientation and for both powder and single-crystal samples. Furthermore, the dHvA frequency spectra have numerous features and could be used (in conjunction with other measurements) to resolve even more complicated structures. Although magnetic measurements under different angles are required for this, having single-crystal samples is not mandatory, a condition that greatly improves the feasibility of high-pressure studies. We have presented the calculated dHvA spectra of structures previously suggested as low- T phases of Li. These data can be used in the analysis of future dHvA measurements for structure determination of Li; a comparison with existing data does not support the thesis that $9R$ is the structure of the Li low- T state.

We expect this paper will stimulate further studies where Fermiology measurements are used for structure determination. Indeed, advances in high-magnetic-field technology in user facilities currently allow generation of magnetic fields in excess of 100 T. These are over six times higher than those used previously to study the FS of lithium. Together with the development of insulating high-pressure cells for Fermiology at high magnetic fields (29), studies at high pressure are a very promising approach that would allow better identification of the complex high-pressure and low-temperature structures of lithium and other metals.

supported by the Energy Frontier Research in Extreme Environments Center, an Energy Frontier Research Center funded by the US Department of Energy (DOE), Office of Science under Award DE-SC0001057, and by Lawrence Livermore National Laboratory (LLNL). The work at LLNL was performed under the auspices of the US DOE under Contract DE-AC52-07NA27344. Computational resources were provided by ACEnet. The experimental works were performed at HPCAT (Sector 16), APS, Argonne National Laboratory. Beam time for these experiments was provided by the Carnegie-DOE Alliance

Center, which is supported by DOE-National Nuclear Security Administration (NNSA) under Grant DE-NA-0002006. HPCAT operations are supported by DOE-NNSA under Award DE-NA0001974 and DOE-Basic Energy Sciences under Award DE-FG02-99ER45775, with partial instrumentation funding by NSF. The APS is a US DOE Office of Science User Facility operated for the DOE Office of Science by Argonne National Laboratory under Contract DE-AC02-06CH11357. The research at University of Utah was supported by National Science Foundation Division of Materials Research Award 1351986.

1. Neaton JB, Ashcroft NW (1999) Pairing in dense lithium. *Nature* 400:141–144.
2. Ashcroft NW (1989) Quantum-solid behavior and the electronic structure of the light alkali metals. *Phys Rev B* 39:10552–10559.
3. Guillaume CL, et al. (2011) Cold melting and solid structures of dense lithium. *Nat Phys* 7:211–214.
4. Tuoriniemi J, et al. (2007) Superconductivity in lithium below 0.4 millikelvin at ambient pressure. *Nature* 447:187–189.
5. Matsuoka T, Shimizu K (2009) Direct observation of a pressure-induced metal-to-semiconductor transition in lithium. *Nature* 458:186–189.
6. Tambllyn I, Raty JY, Bonev SA (2008) Tetrahedral clustering in molten lithium under pressure. *Phys Rev Lett* 101:075703.
7. Lazicki A, Fei Y (2010) High-pressure differential thermal analysis measurements of the melting curve of lithium. *Solid State Commun* 150:625–627.
8. Gorelli FA, et al. (2012) Lattice dynamics of dense lithium. *Phys Rev Lett* 108:055501.
9. Schaeffer AM, et al. (2015) Boundaries for martensitic transition of 7Li under pressure. *Nat Commun* 6:8030.
10. Hanfland M, Syassen K, Christensen NE, Novikov DL (2000) New high-pressure phases of lithium. *Nature* 408:174–178.
11. Shimizu K, Ishikawa H, Takao D, Yagi T, Amaya K (2002) Superconductivity in compressed lithium at 20 K. *Nature* 419:597–599.
12. Schaeffer AMJ, Talmadge WB, Temple SR, Deemyad S (2012) High pressure melting of lithium. *Phys Rev Lett* 109:185702.
13. Elatresh SF, Bonev SA, Gregoryanz E, Ashcroft NW (2016) Role of quantum ion dynamics in the melting of lithium. *Phys Rev B* 94:104107.
14. Matsuoka T, et al. (2014) Pressure-induced reentrant metallic phase in lithium. *Phys Rev B* 89:144103.
15. Barrett CS (1947) A low temperature transformation in lithium. *Phys Rev* 72:245–245.
16. Barrett CS (1956) X-ray study of the alkali metals at low temperatures. *Acta Crystallogr* 9:671–677.
17. McCarthy CM, Tompson CW, Werner SA (1980) Anharmonicity and the low-temperature phase in lithium metal. *Phys Rev B* 22:574–580.
18. Overhauser AW (1984) Crystal structure of lithium at 4.2 K. *Phys Rev Lett* 53:64–65.
19. Smith HG (1987) Martensitic phase transformation of single-crystal lithium from bcc to a 9R-related structure. *Phys Rev Lett* 58:1228–1231.
20. Smith HG (1990) Pressure effects on the martensitic transformation in metallic lithium. *Phys Rev B* 41:1231–1234.
21. Schwarz W, Blaschko O (1990) Polytype structures of lithium at low temperatures. *Phys Rev Lett* 65:3144–3147.
22. Olinger B, Shaner JW (1983) Lithium, compression and high-pressure structure. *Science* 219:1071–1072.
23. Boettger JC, Trickey SB (1985) Equation of state and properties of lithium. *Phys Rev B* 32:3391–3398.
24. Boettger JC, Albers RC (1989) Structural phase stability in lithium to ultrahigh pressures. *Phys Rev B* 39:3010–3014.
25. Staikov P, Kara A, Rahman TS (1997) First-principles studies of the thermodynamic properties of bulk Li. *J Phys Condens Matter* 9:2135.
26. Liu AY, Quong AA, Freericks JK, Nicol EJ, Jones EC (1999) Structural phase stability and electron-phonon coupling in lithium. *Phys Rev B* 59:4028–4035.
27. Shoenberg D (1984) *Magnetic Oscillations in Metals* (Cambridge Univ Press, Cambridge, UK).
28. Hunt MB, Reinders PHP, Springford M (1989) A de Haas-van Alphen effect study of the fermi surface of lithium. *J Phys Condens Matter* 1:6589–6602.
29. Graf DE, Stillwell RL, Purcell KM, Tozer SW (2011) Nonmetallic gasket and miniature plastic turnbuckle diamond anvil cell for pulsed magnetic field studies at cryogenic temperatures. *High Press Res* 31:533–543.
30. Gonze X, et al. (2009) ABINIT: First-principles approach to material and nanosystem properties. *Comput Phys Commun* 180:2582–2615.
31. Hartwigsen C, Goedecker S, Hutter J (1998) Relativistic separable dual-space Gaussian pseudopotentials from H to Rn. *Phys Rev B* 58:3641.
32. Perdew JP, Burke K, Ernzerhof M (1996) Generalized gradient approximation made simple. *Phys Rev Lett* 77:3865–3868.
33. Rourke P, Julian S (2012) Numerical extraction of de haas-van alphen frequencies from calculated band energies. *Comput Phys Commun* 183:324–332.
34. Kokalj A (2003) Computer graphics and graphical user interfaces as tools in simulations of matter at the atomic scale. *Comput Mater Sci* 28:155–168.